

Solar air heater performance prediction using artificial neural network technique with relevant input variables

HARISH KUMAR GHRITLAHRE*
PURVI CHANDRAKAR
ASHFAQUE AHMAD

Department of Energy and Environmental Engineering, Chhattisgarh
Swami Vivekanand Technical University, Bhilai, Chhattisgarh, 491107, India

Abstract Solar air heater (SAH) is an important device for solar energy utilization which is used for space heating, crop drying, timber seasoning etc. Its performance mainly depends on system parameters, operating parameters and meteorological parameters. Many researchers have been used these parameters to predict the performance of SAH by analytical or conventional approach and artificial neural network (ANN) technique, but performance prediction of SAH by using relevant input parameters has not been done so far. Therefore, relevant input parameters have been considered in this study. Total ten parameters were used such as mass flow rate, ambient temperature, wind speed, relative humidity, fluid inlet temperature, fluid mean temperature, plate temperature, wind direction, solar elevation and solar intensity to find out the relevant parameters for ANN prediction. Seven different neural models have been constructed using these parameters. In each model 10 to 20 neurons have been selected to find out the optimal model. The optimal neural models for ANN-I, ANN-II, ANN-III, ANN-IV, ANN-V, ANN-VI and ANN-VII were obtained as 10-17-1, 8-14-1, 6-16-1, 5-14-1, 4-17-1, 3-16-1 and 2-14-1, respectively. It has been found that ANN-II model with 8-14-1 is the optimal model as compared to other neural models. Values of the sum of squared errors, mean relative error, and coefficient of determination were found to be 0.02138, 1.82% and 0.99387, respectively, which shows that the ANN-II developed with mass flow rate, ambient temperature, inlet and mean temperature of air, plate temperature, wind speed and direction, relative humidity, and relevant input parameters performed

*Corresponding Author. Email: harish.ghritlahre@gmail.com

better. The above results show that these eight parameters are relevant for prediction.

Keywords: Artificial neural network; Solar air heater; Thermal performance; Multi-layer perceptron

Nomenclature

A_c	–	collector area, m ²
ANN	–	artificial neural networks
a_i	–	input data
b_j	–	bias
CGP	–	Polak–Ribière conjugate gradient
C_p	–	specific heat, Jkg ⁻¹ K ⁻¹
e	–	roughness size, mm
e/D	–	relative roughness height
I	–	input parameters
I_s	–	solar intensity, W/m ²
LM	–	Levenberg-Marquardt
M	–	model
\dot{m}_f	–	mass flow rate, kg/s
MRE	–	mean relative error
MSE	–	mean square error
MLP	–	multilayered perceptron
O	–	output parameter
OSS	–	one step secant
P/e	–	relative roughness pitch
\dot{Q}_c	–	energy absorbed by collector, W
\dot{Q}_u	–	useful heat gained by air, W
r	–	radiation
R	–	correlation coefficient
RH	–	relative humidity
R^2	–	coefficient of determination
SAH	–	solar air heater
SE	–	solar elevation, (°)
SCG	–	scaled conjugate gradient
SSE	–	sum square error
T	–	temperature, °C
T_n	–	number of training data sets
w_{ij}	–	weights
W_v	–	wind speed, m/s
Y_A	–	actual value
\bar{Y}_A	–	average actual value
Y_P	–	predicted value
\bar{Y}_P	–	average predicted value
WD	–	wind direction, (°)
Z	–	experimental data

Greek symbols

η_{th}	–	thermal efficiency of collector
α	–	arc angle ($^{\circ}$)

Subscripts

a	–	ambient air
d	–	diffuse
fi	–	inlet air
fo	–	outlet air
fm	–	mean air
G	–	global
p	–	plate
min	–	minimum
max	–	maximum

1 Introduction

In recent years, the energy demand is increasing day by day, which is fulfilled by using fossil fuels. But these deposited fossil fuels are limited on the earth, so the demand for energy needs to be utilized by other energy sources. An important role will be played by the renewable energy sources in future for replacement of fossil fuels. In renewable energy sources the solar energy is clean and abundant source of energy. In solar thermal application systems, solar air heater (SAH) is an important device to utilize the solar energy in the form of heat and transmit it to the flowing air. Generally, SAHs are used in space heating, timber seasoning, crop drying applications etc. The conventional SAH performance is very poor because of low heat absorbing capacity, low thermal conductivity of air flowing through the duct and low convective heat transfer coefficient between absorber plate and air. These major issues can be improved by increasing the heat transfer coefficient and heat transfer area. There are various measures to increase the performance of SAHs such as absorbers with artificial roughness, packed/porous bed absorbers and using extended surfaces [1–3].

It has been observed that for performance evaluation of various types of solar air heater systems, researchers used two methods i.e. either mathematical models were developed or expensive experimental studies were conducted. The experimental approach takes more time and the mathematical model requires a programming code to solve the complex equations to find out accurate results [4]. On the other hand, use of artificial neural networks (ANN) saves much time and delivers important information patterns

in a multi-dimensional information domain. Therefore, the ANN technique is very popular in science and engineering sector. Many researchers have used ANN in thermal engineering in the past years [5–39].

ANN is the one of the most commonly used technique due to its fast computing speed and precise results. This technique is widely used for complex problems which are not solved by other conventional approaches. In previous years, ANN technique is more popular in thermal field and it is especially used in solar system performance predictions.

Many researchers have implemented neural technique in the past for performance prediction of various energy systems. Kalogirou applied the ANN technique in the field of renewable energy systems [5]. Hamed *et al.* [6] used ANN technique in water treatment plant to predict the biochemical oxygen demand (BOD) and suspended solids (SS) concentrations. Islamoglu and Kurt developed 4-5-1 neural model to predict the heat transfer in corrugated channels [7]. Kalogirou used neural network technique to evaluate the performance of flat plate collector. To achieve this, six different ANN models were prepared on the basis of measured experimental data and predicted performance with adequate results [8]. Hosoz *et al.* [9] structured 5-5-5 neural model to evaluate performance of cooling tower. They predicted results with the values of correlation coefficient (R): 0.975–0.994, mean relative error (MRE): 0.89–4.64% and very less value of root mean square error (RMSE). Xie *et al.* [10] used ANN model to estimate the heat transfer of shell and tube type heat exchanger. For this, they developed optimal model with 8-6-5-3 neurons and found satisfactory results. Azadeh *et al.* [11] implemented the multilayered perceptron (MLP) model to predict the global solar radiation (GSR) using climatological and metrological variables as input parameters. They collected data from six different cities of Iran. They predicted GSR using 7-4-1 optimal model and reported that the values of mean absolute percentage error (MAPE) and coefficient of determination (R^2) were as 6.70% and 94% respectively. Mohanraj *et al.* [12] created neural structure with 2-12-5 neurons for direct expansion solar-assisted heat pumps and predicted exergetic performance with very low value of RMSE, covariance (COV) and higher value of R . Tan *et al.* [13] used ANN model to predict the performance of compact heat exchanger. Oguz *et al.* [14] developed optimal ANN model of 2-28-2 neurons and predicted the performance of diesel engine using bio-fuels. Chávez-Ramírez *et al.* [15] used ANN technique in the field of fuel cell. They developed 7-6-10-2 neural model with satisfactory results and observed that every output parameter has a maximum error of 9.4% in the

stack voltage prediction and 5.6% from the cathode temperature out. Kamar *et al.* [16] structured 4-3-2 neural model to estimate the performance of automotive air-conditioning systems and observed that the range values of error index, the mean squared error (MSE) and RMSE are 0.65–1.65%, 1.09×10^{-5} – 9.05×10^{-5} and 0.33–0.95%, respectively. Kalogirou *et al.* [17] applied ANN tool and predicted the performance of large solar systems. To achieve this aim, they developed 3-5-5-5-2 neural model and obtained that the value of R^2 for training and testing process were 0.9273 and 0.9327 respectively, which shows the accuracy of the model. Yaici and Entchev developed 10-20-8 neural model to evaluate the performance of a solar thermal energy system utilized for space heating applications and domestic hot water [18]. Esfe *et al.* [19] used ANN method to predict the thermal conductivity of Cu/TiO₂–water/EG hybrid nano fluid and observed the 2-5-5-1 neural model as the optimal model because of lowest values of MSE and mean absolute error (MAE), and highest value of R . Also, they developed the correlation for thermal conductivity prediction on the basis of experimental results. It was also found that ANN model results were better as compare to correlation model. Jani *et al.* [20] applied ANN tool on solid desiccant-vapor compression hybrid air-conditioning system for performance prediction. To achieve this, they structured 12-12-3-3 neural model and got satisfactory results. Mathioulakis *et al.* [21] implemented ANN method to predict the performance of heat pump hot water heaters. They constructed 2-10-6 neural model and trained with LM learning algorithm using collected experimental data, and predicted with less error. Alnaqi *et al.* [22] developed ANN and particle swarm optimization – artificial neural network (PSO-ANN) model to predict the exergetic performance of building integrated PV/T system. They observed that the hybrid model of PSO-ANN performed better as compared to ANN model.

Various researchers used ANN technique in the area of solar energy. Specially for SAHs, the literature review work related to ANN technique has been given in Tab. 1.

Based on literature review, it has been noted that the accuracy of ANN model varies with the parameters taken as input variables. In general, the input variables were selected from the meteorological parameters, systems parameters and operating parameters by various researchers. From Tab. 1, it is clear that different combinations of input variables were selected for neural model for performance prediction and also observed that the input parameters were fixed in all neural models. Therefore, the selection of

Table 1: Summary report of literature survey on application of ANN technique used in solar air heaters.

No.	Author(s)	Neural network type	Neural structure	Input parameters	Algorithm used	Statistical results	Findings
1	Esen <i>et al.</i> [23]	ANN, WNN	6-4-2 6-5-2	$T_{fi}, T_{p1}, T_{p2}, T_{p3}, T_{p4}$	ANN: LM, SCG, CGP WNN: LM	RMSE = 0.0040, 0.0099 $R^2 = 0.9991$	WNN model performed better as compared to ANN model.
2	Cakmak and Yildiz [24]	FFNN	3-10-1	Moisture content, hot air temperature difference, and hot air flow rate	LM	RMSE = 0.0019 MAE = 0.0016 $R = 0.9991$	FFNN model performed better as compared to linear regression model.
3	Caner <i>et al.</i> [25]	MLPNN	8-20-1	M_n , time of measurement, $T_{fi}, T_{fo}, T_{sw}, T_a, T_p$ and I	LM	RMSE = 1.73(%) MAE = 0.9879 $R^2 = 0.9967$	Comparison of the performance of ANN model with step wise regression model. Neural model was a more reliable model for predictions
4	Kamthania <i>et al.</i> [26]	MLPNN	4-15-4	r_d, r_G, T_a and number of clear days	LM	RMSE = 0.10-2.23%	Neural model predicted with accurate results
5	Benli [27]	MLPNN	8-3-1	M_n , data time, $T_{fi}, T_{fo}, \dot{m}, T_a, T_p$, and I	LM	Type I - SSE = 0.0146, $R^2 = 0.9971$. Type II - SSE = 0.0027, $R^2 = 0.9985$.	LM-3 based ANN model was optimal model for prediction.
6	Hamdan <i>et al.</i> [28]	NARX	5-20-5	Initial guess of inside absorber plate surface mean temperature, initial guess of collector back insulation mean surface temperature, initial guess of collector back plate mean surface temperature, initial guess of mean absorber plate temperature and total solar radiation incident on the top of the collector surface	Rprop	RMSE: Training = 1.1872, Testing = 1.0757 R : Training = 0.99997, Testing = 0.999981	NARX model predicted with value of $R = 0.99997$.

continued Tab. 1

7	Ghritlahre and Prasad [29]	MLPNN	4-5-3	\dot{m} , T_a , T_{fi} , and I	LM, SCG, OSS, CGP	$R = 0.9998$	Observation that TRAINLM was optimal training function.
8	Ghritlahre and Prasad [30]	MLPNN	6-6-2	Time of experiments, \dot{m} , T_a , T_{fi} , T_p , and I	LM	For η_{th} : MSE = 3.42E-05, for $R = 0.99678$, and η_{II} : MSE = 1.14E-06, $R = 0.92213$	Prediction with the value of $R = 0.99981$.
9	Ghritlahre and Prasad [31]	MLP, GRNN, RBF and MLR	6-13-1	\dot{m} , T_a , T_{fi} , T_{fm} , W_s and I	LM	For GRNN: RMSE = 5.9284E-06, $R^2 = 0.99758$	ANN models performed better than MLR model.
10	Ghritlahre and Prasad [32]	MLPNN	6-6-1 6-7-1	\dot{m} , e/D , T_a , T_p , T_{fm} , and I	LM, SCG	For LM: MSE = 0.03988, $R^2 = 0.99882$ and SCG: MSE = 4.98182, $R^2 = 0.82485$	The LM learning algorithm was an optimal algorithm.

appropriate relevant input parameters for ANN modeling is an important research gap which has not been considered by any researchers in the past. In the present paper, relevant input parameters have been used to develop the ANN model for performance prediction of SAH. This is the novelty of the present paper.

In view of the above, for optimum prediction of performance MLP model has been developed with relevant input parameters. To achieve this target, experiments were conducted at Jamshedpur city using two different types of absorber plate: arc shaped wire rib roughened and smooth plate. Total 210 data sets were collected from experimental data and calculated values. Ten parameters were used to select the relevant parameters. The main objectives of this paper are: (1) To develop neural model for prediction of thermal performance of SAH. (2) Find out the relevant input parameters.

2 Experimental study and data collection

Figure 1 shows the schematic diagram of experimental setup of present work. The SAH duct is constructed with entrance section, exit section and

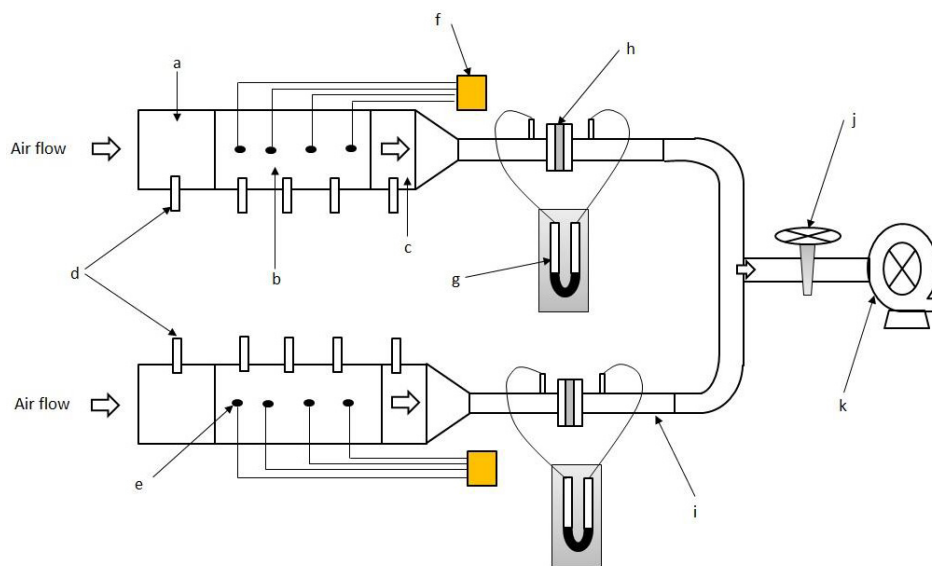


Figure 1: Design of experimental setup: a – entrance section, b – test section, c – exit section, d – digital thermometer, e – thermocouple probe, f – digital display unit, g – manometer, h – orifice meter, i – GI pipe, j – control valve, k – suction blower.

test section. The components used in present setup are absorber plate, glass cover, galvanized iron (GI) pipe connected with exit section, U-tube manometer, orifice plate, valve, suction blower, thermometers. The dimension of duct is $2300\text{ mm} \times 330\text{ mm} \times 35\text{ mm}$ and the exit section is connected with GI pipe of 6.35 cm diameter as shown in Fig. 1. In the test section, absorber plate with black painted GI sheet is used, and this test section is covered with 4 mm glass cover. The photographic view of setup is given in Fig. 2 and the structure of test section shown in Fig. 3. For measurement of mass flow rate the orifice plate has been used. U-tube manometer is fitted across the orifice plate for measurement of pressure drop. The photographic view of absorber plate is shown in Fig. 4, which is 1 mm GI sheet.



Figure 2: Pictorial view of SAH experimental setup.

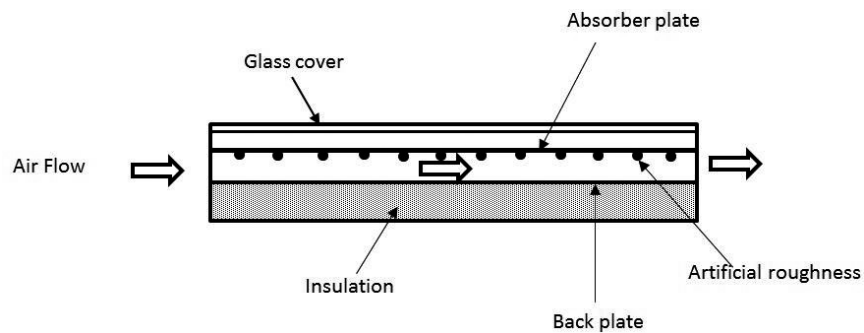


Figure 3: Design of test section.

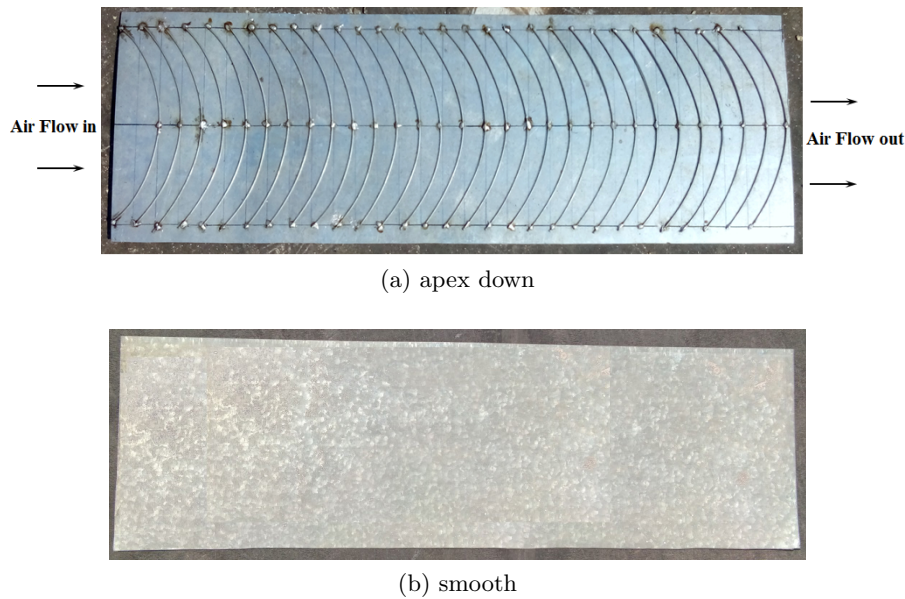


Figure 4: Pictorial view of absorber plates.

Its specification is given in Tab. 2. The experiments have been carried out with various mass flow rates from 0.0070 to 0.0222 kg/s. A 5 HP/3-phase suction blower was used to carry air through the SAH duct. A digital pyranometer was used for the solar intensity measurement and its photographic view is shown in Fig. 5.

Table 2: Parameters considered in the present work.

Ser. no.	Parameters	Value(s)
Operating parameter		
1	Mass flow rate (\dot{m}_f)	0.0070 to 0.0222 kg/sec
Roughness parameters		
2	Relative roughness pitch (P/e)	10
3	Relative roughness height (e/D)	0.0395
4	Roughness height (e)	2.5 mm
5	Arc angle (α)	60°

For measurement of the temperatures at various segments of absorber plates and flowing air temperatures at inlet and outlet section digital ther-



Figure 5: Photographic view of digital pyranometer.

pyranometers were used. The experiments were performed at Jamshedpur (India) in the month of February 2017 and data were taken from 09:00 to 16:00 in clear sky days. At six different mass flow rates of air, the data were collected for arc shaped roughened absorber plate and smooth absorber plate SAHs. The data were collected for seven days at interval of 30 minutes. Total 210 sets of data were collected. The details of data sample collection have been shown in Tab. 3.

In the experimentation, various precautions were taken to measure data from instruments to avoid errors, but errors and uncertainties arise while taking data, calibration, observation and reading. The errors that appear during the experiments have a significant impact on the accuracy of experimental study. During the experiments in SAH, various parameters such as temperatures, pressure drop, wind velocity, length, width, diameter of the pipe and solar intensity were measured by relevant instruments. The concept of uncertainty analysis was introduced by Kline and McClintock [41] and is used for uncertainty analysis of the results. The uncertainty values of various measuring instruments are shown in Tab. 4.

Table 3: A sample data, collected on 26th Feb., 2017 (for $\dot{m}_f = 0.0185$ kg/s).

Time (hours)	RH (%)	T_a (°C)	W_v (m/s)	I (W/m ²)	T_i (°C)	WD (°)	SE (°)	T_{o1} (°C)	T_{o2} (°C)	T_{p1} (°C)	T_{p2} (°C)	T_{p3} (°C)	T_{p4} (°C)
09:00	35	20.5	1.3	429.0	24.5	205	30	26.8	29.8	45.5	44.4	43.3	41.1
09:30	29	22.5	0.8	510.4	26.0	191	36	29.3	32.3	48.3	47.1	45.9	43.5
10:00	24	24.2	1.0	538.9	26.7	208	41	31.9	35.0	54.3	52.7	51.2	48.0
10:30	20	25.0	1.1	628.2	30.0	224	46	36.0	39.0	60.9	59.3	57.7	54.4
11:00	19	25.5	0.7	652.6	30.5	171	47	37.0	40.1	63.8	61.9	59.9	56.0
11:30	16	26.8	2.7	712.6	30.8	212	51	37.8	40.9	63.9	62.1	60.3	56.7
12:00	16	27.0	2.2	702.3	32.0	325	55	38.8	41.9	65.4	63.6	61.9	58.3
12:30	16	27.5	2.2	700.6	30.9	287	57	38.5	42.0	65.5	63.6	61.7	57.9
13:00	14	27.7	0.6	726.2	32.7	314	58	39.3	43.0	65.4	63.6	61.8	58.1
13:30	14	29.0	2.1	702.3	33.3	19	57	39.3	42.8	62.4	60.8	59.2	55.9
14:00	13	28.9	1.42	685.4	33.3	7	51	39.4	42.6	61.0	59.6	58.2	55.3
14:30	13	29.0	0.94	649.5	33.3	353	46	38.9	42.1	57.4	56.1	54.8	52.2
15:00	12	29.9	3.70	579.9	32.5	21	41	37.7	40.3	51.9	50.8	49.8	47.6
15:30	14	29.9	2.93	496.0	32.4	36	35	36.8	38.7	47.0	46.3	45.5	44.0
16:00	14	29.3	1.32	400.5	32.1	356	29	35.3	37.3	42.5	42.0	41.5	40.4

Table 4: Uncertainties occurring at the time of data collection.

Ser. no.	Measuring devices/parameters	Value
1	Temperature measurement	
	Collector inlet	± 0.166 °C
	Collector outlet	± 0.166 °C
	Absorber plate	± 0.166 °C
	Ambient air	± 0.166 °C
2	Air velocity measurement	± 0.14 m/s
3	Solar radiation measurement	± 0.1 W/m ²
4	Pressure drop	± 1 mm H ₂ O
5	Vernier calipers	0.0002 m
6	Linear scale	± 1 mm H ₂ O
7	Uncertainty in reading values from table	$\pm 0.1 - 0.2\%$

The uncertainties of main parameters are given as:

$$\begin{array}{l} \dot{m} \quad \pm 0.876 \text{ kg/s} \\ \dot{Q}_u \quad \pm 3.36 \text{ W} \end{array}$$

Considering the relative uncertainties in the individual factors introduced by u_i ($i = 1, \dots, n$), the uncertainty is calculated using the equation [40]

$$U = \left[u_1^2 + u_2^2 + \dots + u_n^2 \right]^{0.5}. \quad (1)$$

3 Performance analysis of solar air heater

The performance of solar air heater is expressed by thermal efficiency, i.e., the ratio of solar energy gained by flowing air to solar energy collected by absorber plate [1, 2]. The performance of SAH is η_{th} represented by the following formula:

$$\eta_{th} = \frac{\dot{Q}_u}{\dot{Q}_c}. \quad (2)$$

The solar energy absorbed by absorber plate and transmitted to the flowing air is

$$\dot{Q}_u = \dot{m}_f C_p \Delta T_f = \dot{m}_f C_p (T_{fo} - T_{fi}). \quad (3)$$

The solar energy received by absorber plate is given by

$$\dot{Q}_c = I_s A_c, \quad (4)$$

where I_s is the rate of radiation incidence per unit area of collector surface and A_c is the absorber plate area.

Thus, the thermal efficiency of solar air heater is expressed by following equation [1, 2]:

$$\eta_{th} = \frac{\dot{m}_f C_p (\Delta T)}{I_s A_c} = \frac{\dot{m}_f C_p (T_{fo} - T_{fi})}{I_s A_c}. \quad (5)$$

4 Artificial neural network

In the field of artificial intelligence (AI), an artificial neural network (ANN) is the most commonly used technique for optimization, simulation, clustering, pattern detection, prediction and to solve nonlinear function. ANN works like a human brain and its structure is similar like human nervous system. The basic structure of biological neurons is shown in Fig. 6. The biological neuron consists with soma/ cell body, synapses, dendrites and axon whose functions are given below [4, 34, 42]:

- *Dendrites*: collects the signals or information.

- *Soma or cell body*: behaves like a processor.
- *Synapses*: it is the link between dendrites and axon.
- *Axon*: it gives the output signal to the other neurons.

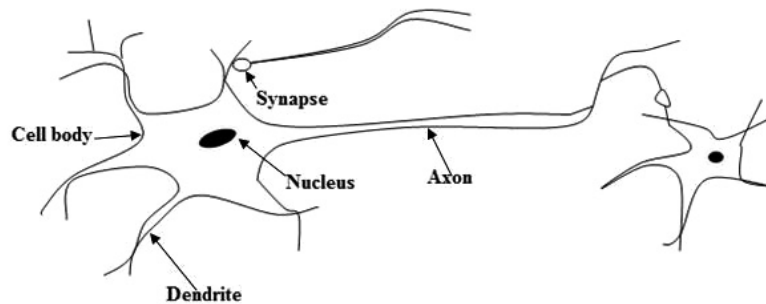


Figure 6: Basic structure of biological neurons.

Basically ANN performs in two steps: first learning and second storing the data sets in weights. ANN tool is mostly used for prediction of data which is mainly based on the parameters used in input layer, the structure of neural model and learning process. For the learning process various algorithms are used which reduce the errors between actual and predicted values by updating weights and biases. The major advantages of ANN technique are solving a complex problem which is not solved by other conventional technique and its processing speed is also very fast.

In general, the MLP model is most commonly used neural model, which is structured with three different layers such as input layer, output layer and hidden layer. Figure 7 shows the general structure of MLP feed forward neural networks. The product of each input signals (a_i) and weights (w_{ij}) is passed through the summing junction and added with bias (b_j), which is expressed by [4, 33–39]

$$X = \sum_{i=1}^n a_i w_{ij} + b_j. \quad (6)$$

For output generation, this sum X goes through the transfer function which is expressed as

$$F(X) = u_j = \left[\sum_{i=1}^n a_i w_{ij} + b_j \right]. \quad (7)$$

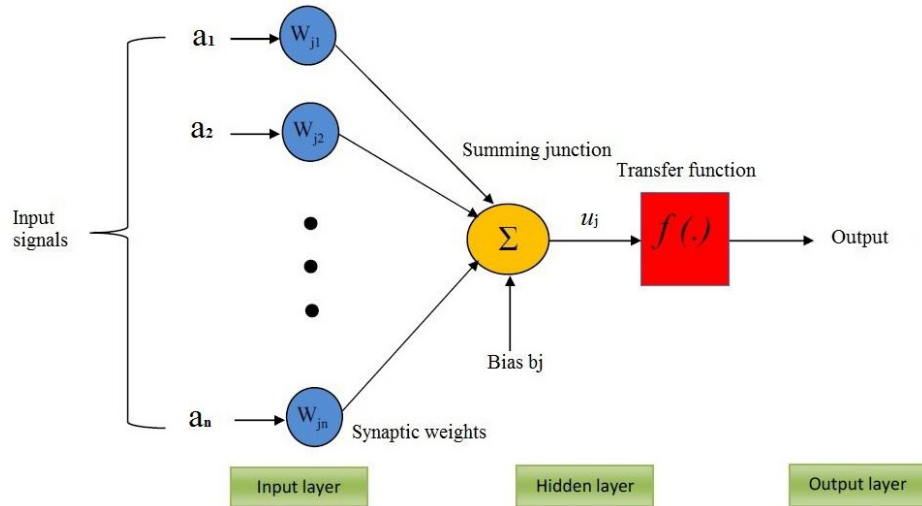


Figure 7: Basic design of the neural structure.

The transfer functions are used in the hidden and output layer. The most commonly used functions are *logsig*, *tansig*, and *purelin*. The *logsig* and *tansig* are nonlinear activation functions which are called as sigmoidal function. The *logsig* transfer function output lies between 0 and 1 which is expressed as following function:

$$F(X) = \frac{1}{1 + \exp(-X)}. \quad (8)$$

If negative values are found in input and output layers, then *tansig* transfer function is preferred and it is given by

$$F(X) = \frac{\exp(X) - \exp(-X)}{\exp(X) + \exp(-X)}. \quad (9)$$

For training process, various types of learning algorithms are used such as: Levenberg-Marquardt (LM), Polak-Ribière conjugate gradient (CGP), one step secant (OSS), scaled conjugate gradient (SCG), and Broyden Fletcher-Goldfarb-Shanno (BFGS) quasi-Newton (BFG), etc. in which, LM is most commonly used algorithm due to its fast computing speed and minimising error [42–44].

5 Selection criteria of optimal ANN model

The performances of neural models were evaluated by using the statistical parameters mean square error (MSE) and correlation coefficient (R). These parameters are calculated by following formula:

Mean square error:

$$\text{MSE} = \frac{1}{n} \sum_{i=1}^n (Y_{A,i} - Y_{P,i})^2. \quad (10)$$

Correlation coefficient:

$$R = \frac{\sum_{i=1}^n (Y_{P,i} - \bar{Y}_P) \cdot (Y_{A,i} - \bar{Y}_A)}{\sqrt{\sum_{i=1}^n (Y_{P,i} - \bar{Y}_P)^2 \sum_{i=1}^n (Y_{A,i} - \bar{Y}_A)^2}}. \quad (11)$$

6 Discussion and analysis of results

6.1 Data collection

In this work, total 210 data sets of SAH were collected from the experiments conducted at National Institute of Technology (NIT) Jamshedpur. Experiments were executed with two different kinds of absorber plate such as roughened absorber plate using arc shaped wire rib and smooth absorber plate as shown in Fig. 4. Ten parameters data were measured from experiments and its range of values is shown in Tab. 5.

Table 5: Range of parameters.

Parameters	Variables symbols and units	Range
<i>Input</i>	Relative humidity, RH (%)	8–45
	Ambient air temperature, T_a ($^{\circ}\text{C}$)	19.5–34.7
	Inlet air temperature, T_{fi} ($^{\circ}\text{C}$)	23.1–38.2
	Mean air temperature, T_{fm} ($^{\circ}\text{C}$)	25.0–44.2
	Plate temperature, T_p ($^{\circ}\text{C}$)	41.3–87.5
	Wind velocity, W_v (m/s)	0.3–4.5
	Mass flow rates, \dot{m} (kg/s)	0.0070–0.0222
	Wind direction, WD ($^{\circ}$)	6–359
	Solar elevation, SE ($^{\circ}$)	28–59
	Solar intensity, I (W/m^2)	360.8–850.3
<i>Output</i>	Thermal efficiency, η_{th}	0.1698–0.6734

6.2 Neural structure development

From the literature study related to ANN technique; it has been observed that the MLP model is most commonly used model. Due to this reason in the present work MLP model has been developed to predict the thermal performance. The proposed neural model developed by using ten parameters such as solar intensity, mass flow rate, wind speed, mean temperature of air, inlet air temperature, plate temperature, relative humidity, wind direction, solar elevation and ambient temperature, and thermal efficiency which is used as output variable in last layer as shown in Fig. 8. Out of 210 data sets, 80% data were taken for training, 10% for testing and remaining 10% for validation. All the experimental data sets were normalized between 1 and -1 before the development of neural structure. Data sets were for normalized by using the following equation [36].

$$Z = \frac{Z_i - Z_{\min}}{Z_{\max} - Z_{\min}} 2 + (-1). \quad (12)$$

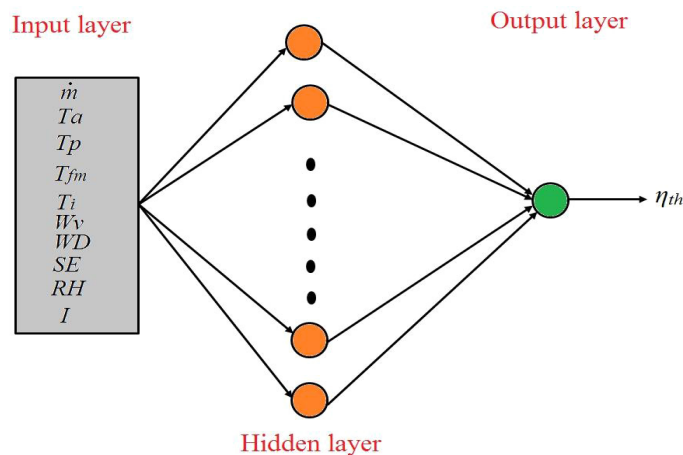


Figure 8: Proposed neural model.

Transfer function is an important function to develop a neural model, which is used for determining the sum of weighted inputs and bias to produce the final output. In this study, tansig and purelin transfer function were used in hidden and output layer respectively. There are many types of learning algorithms are used for training of neural model such as LM, SCG, CGP,

OSS etc. in which LM is most popular algorithm used for training [43]. Due to this reason, LM algorithm is used in present study.

The main objective of this study is to predict the thermal performance using relevant input parameters. To achieve this aim, seven different ANN models have been structured with ten different parameters as given in Tab. 6. The hidden layer required neurons to complete the development of neural structure. So, these numbers of neurons were calculated from the equation

$$H_n = \frac{I + O}{2} + \sqrt{T_n}, \quad (13)$$

where I and O are input and output parameters respectively, and T_n is a number of training data sets.

Table 6: Proposed neural models.

Ser. No.	Neural model	Input parameters
1	ANN-I	$m, T_a, T_{fi}, T_{fm}, T_{pm}, W_v, RH, I, WD, SE$
2	ANN-II	$m, T_a, T_{fi}, T_{fm}, T_{pm}, W_v, RH, I$
3	ANN-III	$m, T_{fi}, T_{fm}, T_{pm}, W_v, I$
4	ANN-IV	$T_a, T_{fi}, T_{fm}, W_v, I$
5	ANN-V	$RH, T_{fi}, T_{fm}, T_{pm}$
6	ANN-VI	T_{fi}, T_{pm}, I
7	ANN-VII	T_a, T_{pm}

From Eq. (13), it has been observed that 19, 14, 17, 16, 16, 15 and 15 number of hidden neurons were obtained for ANN-I, ANN-II, ANN-III, ANN-IV, ANN-V, ANN-VI and ANN-VII respectively. Due to this reason 10 to 20 number of neurons were selected for all above models to develop the optimal neural structure.

6.3 ANN simulation result

All neural models have been trained with LM learning algorithm using 10 to 20 numbers of hidden neurons. The performance of models is analyzed on the basis of statistical error analysis. The statistical error analysis of different models is given in Tabs. 7–13. From these tables, it is clear that optimal model is found at the minimum value of MSE and maximum values of R .

Table 7: Statistical analysis of ANN with 10- H_n -1.

	H_n	R_1	R_2	R_3	R	MSE
Input parameters = 10	10	0.98050	0.96851	0.97925	0.97822	0.000867
	11	0.98837	0.98120	0.96648	0.98584	0.000674
	12	0.99175	0.98520	0.98125	0.98915	0.000591
	13	0.98476	0.98641	0.96005	0.98350	0.000694
	14	0.99559	0.95748	0.96837	0.99036	0.000646
	15	0.99149	0.96989	0.94818	0.98270	0.001320
	16	0.98764	0.98245	0.97901	0.98526	0.000681
	17	0.99619	0.98863	0.98411	0.99366	0.000389
	18	0.99323	0.98112	0.94699	0.98641	0.001002
	19	0.99001	0.96701	0.97407	0.98701	0.000624
	20	0.98573	0.97551	0.9655	0.98124	0.000954

Table 8: Statistical analysis of ANN with 8- H_n -1.

	H_n	R_1	R_2	R_3	R	MSE
Input parameters = 8	10	0.97749	0.96635	0.91478	0.97129	0.001619
	11	0.99282	0.97285	0.96911	0.9885	0.000732
	12	0.99603	0.99071	0.95016	0.98963	0.000850
	13	0.99551	0.98756	0.98547	0.99321	0.000411
	14	0.99858	0.99322	0.98857	0.99694	0.000233
	15	0.9936	0.99056	0.99069	0.99277	0.000309
	16	0.99129	0.9782	0.98691	0.9894	0.000521
	17	0.99365	0.95014	0.9727	0.98758	0.000886
	18	0.99037	0.99312	0.96407	0.98757	0.000647
	19	0.98921	0.95993	0.96901	0.98481	0.000774
	20	0.98618	0.98005	0.97513	0.98383	0.001036

Table 9: Statistical analysis of ANN with 6- H_n -1.

	H_n	R_1	R_2	R_3	R	MSE
Input parameters = 6	10	0.99001	0.98653	0.97936	0.98816	0.000588
	11	0.99258	0.99058	0.98509	0.99163	0.001382
	12	0.98396	0.97295	0.98221	0.98242	0.000712
	13	0.99158	0.98295	0.96312	0.98825	0.001501
	14	0.99029	0.99017	0.98531	0.9905	0.001121
	15	0.992	0.98695	0.95918	0.98836	0.000707
	16	0.99541	0.99172	0.98548	0.99336	0.000404
	17	0.98969	0.98676	0.97983	0.98836	0.000474
	18	0.96676	0.97739	0.94128	0.96543	0.001463
	19	0.98729	0.96667	0.95922	0.98347	0.000796
	20	0.98976	0.98772	0.98036	0.98831	0.000530

Table 10: Statistical analysis of ANN with 5- H_n-1 .

	H_n	R_1	R_2	R_3	R	MSE
Input parameters = 5	10	0.86887	0.75161	0.76783	0.84193	0.007472
	11	0.83863	0.70309	0.72045	0.80595	0.008776
	12	0.72982	0.82666	0.72528	0.73953	0.007306
	13	0.80596	0.81058	0.77967	0.80668	0.005443
	14	0.87007	0.85855	0.87247	0.87177	0.004374
	15	0.79921	0.67704	0.76288	0.77905	0.007193
	16	0.81772	0.75592	0.67929	0.79728	0.007163
	17	0.76512	0.69955	0.59109	0.74766	0.006963
	18	0.81452	0.66574	0.68064	0.77603	0.009682
	19	0.77478	0.6672	0.51906	0.74224	0.009548
	20	0.80475	0.70725	0.79304	0.79413	0.006585

Table 11: Statistical analysis of ANN with 4- H_n-1 .

	H_n	R_1	R_2	R_3	R	MSE
Input parameters = 4	10	0.89332	0.88074	0.70458	0.86278	0.007005
	11	0.8878	0.9183	0.83724	0.88122	0.004767
	12	0.86136	0.90672	0.77561	0.8609	0.004168
	13	0.83185	0.80741	0.85114	0.83029	0.005196
	14	0.80167	0.9067	0.87551	0.81531	0.004970
	15	0.89104	0.91322	0.88665	0.89201	0.003269
	16	0.88359	0.89067	0.86768	0.88119	0.004307
	17	0.89349	0.91954	0.91944	0.89704	0.003019
	18	0.85334	0.85489	0.88457	0.84955	0.004900
	19	0.88435	0.89731	0.83538	0.88016	0.004193
	20	0.86857	0.93575	0.83525	0.87124	0.004523

Table 12: Statistical analysis of ANN with 3- H_n-1 .

	H_n	R_1	R_2	R_3	R	MSE
Input parameters = 3	10	0.89988	0.91355	0.88565	0.90029	0.003296
	11	0.89424	0.86464	0.91519	0.89222	0.003769
	12	0.89456	0.88269	0.86801	0.88758	0.003757
	13	0.92365	0.91091	0.85486	0.91432	0.003607
	14	0.89346	0.8818	0.87339	0.88991	0.003939
	15	0.88067	0.89643	0.87148	0.87921	0.004759
	16	0.94163	0.91783	0.92429	0.92819	0.002529
	17	0.88352	0.88945	0.84557	0.87988	0.003863
	18	0.90952	0.90919	0.87112	0.90431	0.003863
	19	0.90718	0.89653	0.89994	0.9034	0.003647
	20	0.91306	0.90146	0.81301	0.90188	0.004151

Table 13: Statistical analysis of ANN with 2- H_n -1.

	H_n	R_1	R_2	R_3	R	MSE
Input parameters = 2	10	0.69977	0.75887	0.56942	0.69311	0.008609
	11	0.70809	0.76438	0.50251	0.69957	0.009235
	12	0.68493	0.77312	0.65601	0.69046	0.008340
	13	0.66698	0.60066	0.65691	0.65636	0.011852
	14	0.74575	0.82986	0.69322	0.74489	0.007960
	15	0.70735	0.71701	0.67192	0.69961	0.009959
	16	0.70048	0.62762	0.64262	0.68131	0.011047
	17	0.68336	0.6424	0.58581	0.66912	0.010288
	18	0.72986	0.77515	0.6405	0.71718	0.010313
	19	0.68281	0.65167	0.50328	0.65589	0.011314
20	0.68341	0.60015	0.53164	0.65458	0.011844	

From Tab. 14, it has been observed that the ANN model with 8-14-1 neurons is the optimal model due to lowest error (MSE = 0.000233) and highest values of correlation coefficient ($R = 0.99964$).

Table 14: Optimal neural models.

Ser. No.	Neural model	Optimal structure	MSE	R	Remarks
1	ANN-I	10-17-1	3.89E-04	0.99366	Optimal models are obtained on the basis of minimum value of MSE and maximum values of R .
2	ANN-II	8-14-1	2.33E-04	0.99694	
3	ANN-III	6-16-1	4.04E-04	0.99336	
4	ANN-IV	5-14-1	4.37E-03	0.87177	
5	ANN-V	4-17-1	3.01E-03	0.89704	
6	ANN-VI	3-16-1	2.52E-03	0.92819	
7	ANN-VII	2-14-1	7.69E-03	0.74489	

The performance curve of ANN-II model is shown in Fig. 9. It is clear that the MSE values are decreasing with increase in the epoch. The training process is stopped at epoch 51 as the minimum MSE of the validating sets was obtained. The best validation performance occurred at epoch 45 and MSE during validation was found to be 0.00021534. The regression plot of optimal ANN-II is shown in Fig. 10. From this figure, it has been found that the values of R of training, testing, validation and all processes are 0.99858, 0.98857, 0.99322 and 0.99694 respectively, which are showing that the actual values of experimental data matches with the ANN predicted output data.

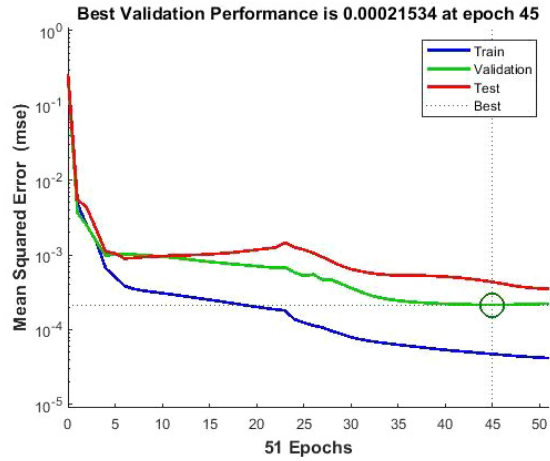


Figure 9: Performance curve of ANN-II.

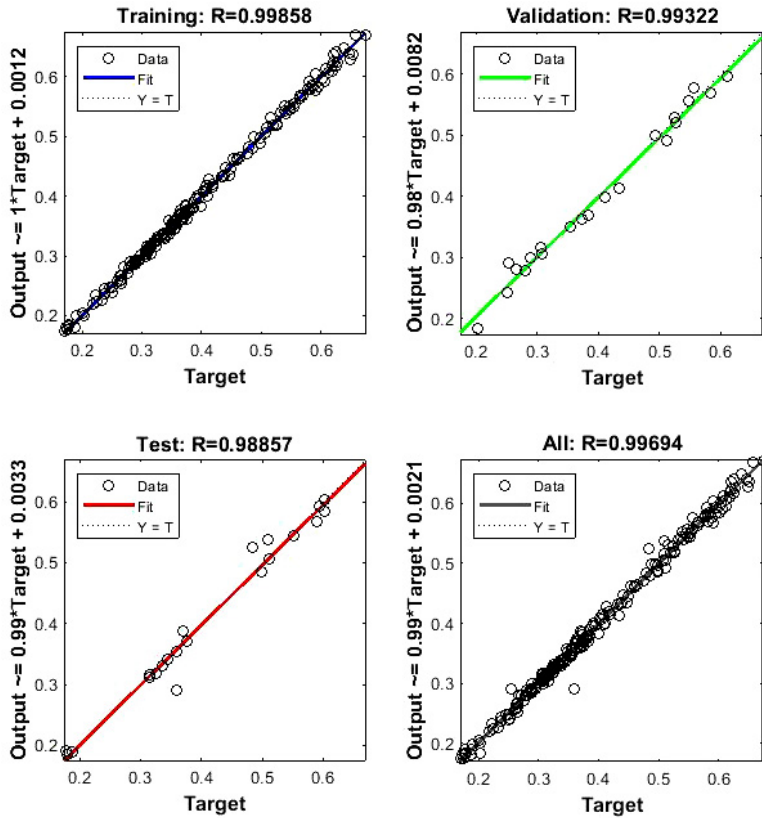


Figure 10: Regression plot of ANN-II.

The comparison graph of ANN-II model between actual and predicted data is shown in Fig. 11. The upper curve is for roughened SAH and lower curve is for the flat plate SAH. The individual error of each sample is shown in Fig. 12 and its histogram graph is shown in Fig. 13. Here, it is evident

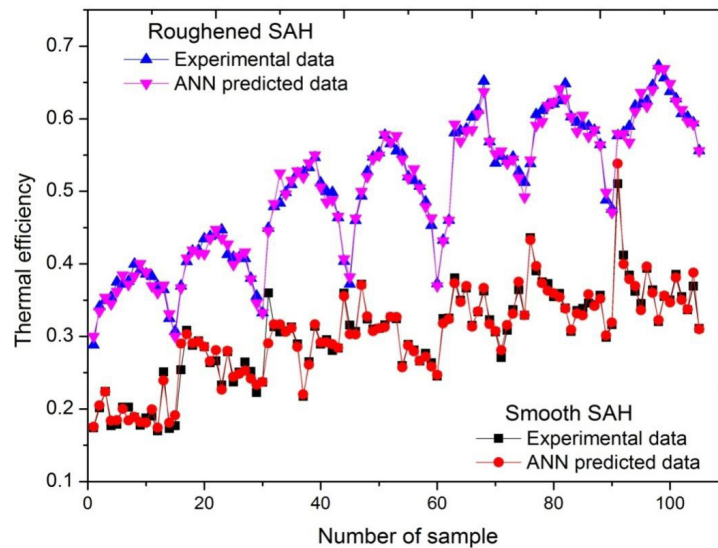


Figure 11: Comparative graph between ANN-II predictions and actual experimental data.

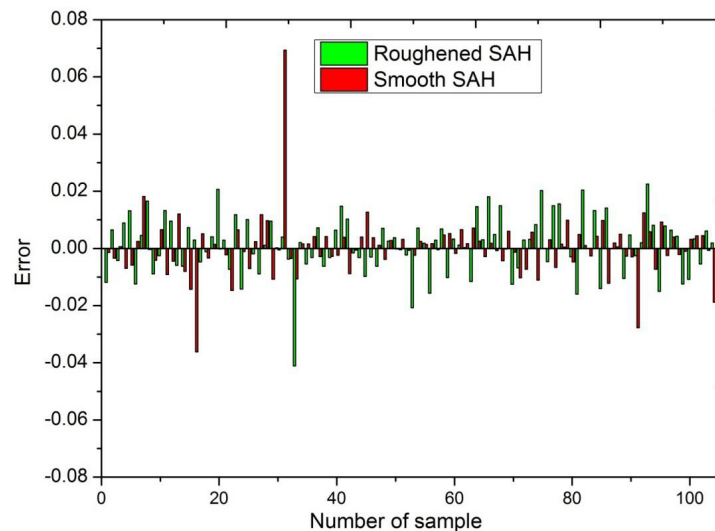


Figure 12: Individual errors graph of ANN-II.

that over 43% errors are accumulated between 0–0.005 for roughened SAH and in case of smooth SAH 46% error 0.005 to 0.01 are accumulated. The performance of ANN-II model has been evaluated on the basis of statistical error analysis which is given in Fig. 14. It has been found that the values

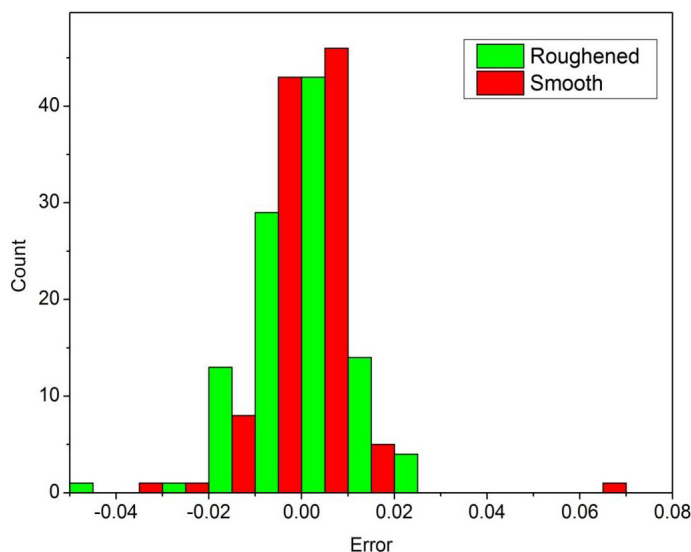


Figure 13: Histogram error of ANN-II.

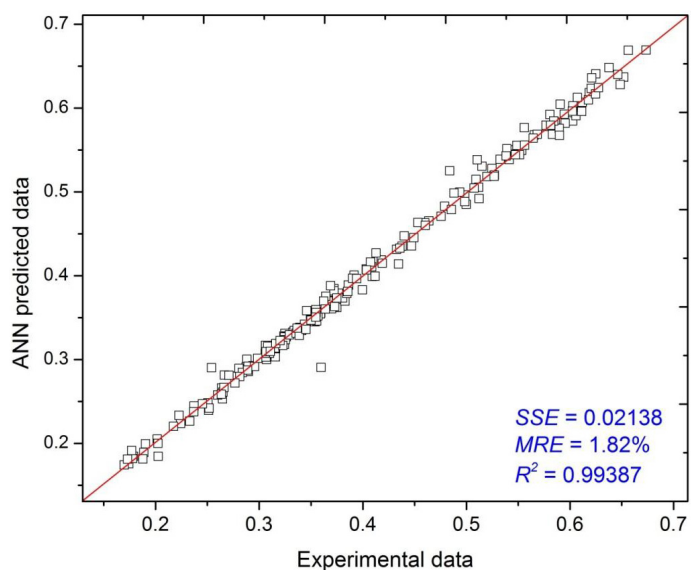


Figure 14: Regression plot of ANN-II.

of SSE and MRE are 0.02138 and 1.82%, respectively, and the value of R^2 is obtained as 0.99387. These results show that the ANN-II model with eight parameters is the most appropriate model to predict the thermal performance of SAH.

7 Conclusion

In the present work, artificial neural network (ANN) technique is used to predict the thermal performance of solar air heater (SAH) using relevant input parameters. For accurate prediction, seven different neural models were developed with parameters such as mass flow rate, ambient temperature, inlet and mean temperature of air, plate temperature, wind speed and direction, relative humidity, and relevant input parameters. The neural models have been evaluated on the basis statistical error analysis using the parameters with the mean square error (MSE) and correlation coefficient (R). The following conclusions have been drawn from this presented work:

- (i) The multilayered perceptron (MLP) model has been used to predict the performance.
- (ii) 10 to 20 numbers of hidden neurons were used in all models to find out the optimal neural model.
- (iii) The optimal neural models were obtained for ANN-I, ANN-II, ANN-III, ANN-IV, ANN-V, ANN-VI and ANN-VII with neurons 10-17-1, 8-14-1, 6-16-1, 5-14-1, 4-17-1, 3-16-1 and 2-14-1 respectively.
- (iv) ANN-II model obtained as best model as compared to others neural models.
- (v) The values of mean relative error (MRE) and sum of squared errors (SSE) are 1.82% and 0.02138, respectively, for ANN-II.

Acknowledgment The Authors would like to extend their special thanks to NIT Jamshedpur and Department of Mechanical Engineering for helping in experimental work and necessary laboratory facility.

References

- [1] SUKHATME S.P., NAYAK J.K.: *Solar Energy. Principles of Thermal Collection and Storage*. Tata McGraw Hill, New Delhi 1996.
- [2] DUFFIE J.A., BECKMAN W.A.: *Solar Engineering of Thermal Processes* (3rd Edn.). Wiley Interscience, New York 2006.
- [3] GHRTLAHRE H.K.: *Performance evaluation of solar air heating systems using artificial neural network*. PhD thesis, National Institute of Technology, Jamshedpur, India, 2019.
- [4] HAYKIN S.: *Neural Networks: A Comprehensive Foundation*. Macmillan, New York 1994.
- [5] KALOGIROU S.A.: *Artificial neural networks in renewable energy systems applications: a review*. *Renew. Sustain. Energy Rev.* **5**(2001), 373–401.
- [6] HAMED M.M., KHALAFALLAH M.G., HASSANIEN E.A.: *Prediction of wastewater treatment plant performance using artificial neural networks*. *Environ. Model. Softw.* **19**(2004), 10, 919–928.
- [7] ISLAMOGLU Y., KURT A.: *Heat transfer analysis using ANNs with experimental data for air flowing in corrugated channels*. *Int. J. Heat Mass Tran.* **47**(2004), 1361–1365.
- [8] KALOGIROU S.A.: *Prediction of flat-plate collector performance parameters using artificial neural networks*. *Sol. Energy* **80**(2006), 3, 248–259.
- [9] HOSOZ M., ERTUNC H.M., BULGURCU H.: *Performance prediction of a cooling tower using artificial neural network*. *Energ. Convers. Manage.* **48**(2007), 1349–59.
- [10] XIE H., LIU L., MA F., FAN H.: *Performance prediction of solar collectors using artificial neural networks*. In: *Proc. Int. Conf. on Artificial Intelligence and Computational Intelligence* (2009) DOI: 10.1109/AICI.2009.344.
- [11] AZADEH A., MAGHSOUDI A., SOHRABKHANI S.: *An integrated artificial neural networks approach for predicting global radiation*. *Energ. Convers. Manage.* **50**(2009), 6, 1497–1505.
- [12] MOHANRAJ M., JAYARAJ S., MURALEEDHARAN C.: *Exergy analysis of direct expansion solarassisted heat pumps using artificial neural networks*. *Int. J. Energy Res.* **33**(2009), 1005–1020.
- [13] TAN C.K., WARD J., WILCOX S.J., PAYNE R.: *Artificial neural network modelling of the thermal performance of a compact heat exchanger*. *Appl. Therm. Eng.* **29**(2009), 17–18, 3609–3617.
- [14] OĞUZ H., SARITAS I., BAYDAN H.E.: *Prediction of diesel engine performance using biofuels with artificial neural network*. *Expert Syst. Appl.* **37**(2010), 9, 6579–6586.
- [15] CHÁVEZ-RAMÍREZ A.U., MUÑOZ-GUERRERO R., DURÓN-TORRES S.M., FERRARO M., BRUNACCINI G., SERGI F., ANTONUCCI V., ARRIAGAA L.G.: *High power fuel cell simulator based on artificial neural network*. *Int. J. Hydrogen Energ.* **35**(2010), 21, 12125–12133.
- [16] KAMAR H.M., AHMAD R., KAMSAH N.B., MUSTAFA A.F.M.: *Artificial neural networks for automotive air-conditioning systems performance prediction*. *Appl. Therm. Eng.* **50**(2013), 1, 63–70.

- [17] KALOGIROU S.A., MATHIOULAKIS E., BELESSIOTIS V.: *Artificial neural networks for the performance prediction of large solar systems*. *Renew. Energy* **63**(2014), 90–97.
- [18] YAİCI W., ENTCHEV E.: *Performance prediction of a solar thermal energy system using artificial neural networks*. *Appl. Therm. Eng.* **73**(2014), 1348–1359.
- [19] ESFE M.H., WONGWISES S., NADERI A., ASADI A., SAFAEI M.R., ROSTAMIAN H., DAHARI M., KARIMPOUR A.: *Thermal conductivity of Cu/TiO₂-water/EG hybrid nanofluid: Experimental data and modeling using artificial neural network and correlation*. *Int. Commun. Heat Mass* **66** (2015), 100–104.
- [20] JANI D.B., MISHRA M., SAHOO P.K.: *Performance prediction of solid desiccant – vapor compression hybrid air-conditioning system using artificial neural network*. *Energy* **103**(2016), 618–629.
- [21] MATHIOULAKIS E., PANARAS G., BELESSIOTIS V.: *Artificial neural networks for the performance prediction of heat pump hot water heaters*. *Int. J. Sust. Energy* **37**(2018), 2, 173–192.
- [22] ALNAQI A.A., MOAYEDI H., SHAHSAVAR A., NGUYEN T.K.: *Prediction of energetic performance of a building integrated photovoltaic/ thermal system thorough artificial neural network and hybrid particle swarm optimization models*. *Energ. Convers. Manage.* **183**(2019), 137–148.
- [23] ESEN H., OZGEN F., ESEN M., SENGUR A.: *Artificial neural network and wavelet neural network approaches for modelling of a solar air heater*. *Expert Syst. Appl.* **36**(2009), 11240–11248.
- [24] CAKMAK G., YILDIZ C.: *The prediction of seedy grape drying rate using a neural network method*. *Comput. Electron. Agric.* **75**(2011), 132–138.
- [25] CANER M., GEDIK E., KEÇEBAS A.: *Investigation on thermal performance calculation of two type solar air collectors using artificial neural network*. *Expert Syst. Appl.* **38**(2011), 1668–74.
- [26] KAMTHANIA D., TIWARI G.N.: *Performance analysis of a hybrid photovoltaic thermal double pass air collector using ANN*. *Appl. Sol. Energy* **48**(2012), 3, 186–192.
- [27] BENLI H.: *Determination of thermal performance calculation of two different types solar air collectors with the use of artificial neural networks*. *Int. J. Heat Mass Tran.* **60**(2013), 1–7.
- [28] HAMDAN M.A., ABDELHAFEZ E.A., HAMDAN A.M., HAJKHALIL R.A.: *Heat transfer analysis of a flat-plate solar air collector by using an artificial neural network*. *J. Infrastruct. Syst.* 2014. DOI: 10.1061/(ASCE)IS.1943-555X.0000213.
- [29] GHRITLAHRE H.K., PRASAD R.K.: *Prediction of thermal performance of unidirectional flow porous bed solar air heater with optimal training function using Artificial Neural Network*. *Energy Proced.* **109**(2017), 369–376.
- [30] GHRITLAHRE H.K., PRASAD R.K.: *Energetic and exergetic performance prediction of roughened solar air heater using artificial neural network*. *Ciência e Técnica Vitivinícola* **32**(2017), 11, 2–24.
- [31] GHRITLAHRE H.K., PRASAD R.K.: *Investigation of thermal performance of unidirectional flow porous bed solar air heater using MLP, GRNN, and RBF models of ANN technique*. *Therm. Sci. Eng. Progress* **6**(2018), 226–235.

- [32] GHRITLAHRE H.K., PRASAD R.K.: *Development of optimal ANN model to estimate the thermal performance of roughened solar air heater using two different learning algorithms*. Annals of Data Science **5**(2018), 3, 453–467.
- [33] GHRITLAHRE H.K.: *Development of feed-forward back-propagation neural model to predict the energy and exergy analysis of solar air heater*. Trends Renew. Energ. **4**(2018), 213–235. DOI: 10.17737/tre.2018.4.2.0078.
- [34] GHRITLAHRE H.K., PRASAD R.K.: *Application of ANN technique to predict the performance of solar collector systems – A review*. Renew. Sust. Energ. Rev. **84**(2018), 75–88.
- [35] GHRITLAHRE H.K., PRASAD R.K.: *Exergetic performance prediction of roughened solar air heater using artificial neural network*. Strojnikivestnik – J. Mech. Eng. **64**(2018), 3, 195–206.
- [36] GHRITLAHRE H.K., PRASAD R.K.: *Investigation on heat transfer characteristics of roughened solar air heater using ANN technique*. IJHT **36**(2018), 1, 102–110.
- [37] GHRITLAHRE HK, PRASAD RK.: *Prediction of heat transfer of two different types of roughened solar air heater using Artificial Neural Network technique*. Therm. Sci. Eng. Prog. **8**(2018), 145–153.
- [38] GHRITLAHRE H.K., PRASAD R.K.: *Exergetic performance prediction of solar air heater using MLP, GRNN and RBF models of artificial neural network technique*. J. Environ. Manage. **223**(2018), 566–575.
- [39] GHRITLAHRE H.K., PRASAD R.K.: *Prediction of exergetic efficiency of arc shaped wire roughened solar air heater using ANN model*. IJHT **36**(2018), 3, 1107–1115.
- [40] HOLMAN J.P.: *Experimental Methods for Engineers*. McGraw-Hill, New York 2007.
- [41] KLINE S.J., MCCLINTOCK F.A.: *Describe uncertainties in single sample experiments*. Mech. Eng. (1953), 3–8.
- [42] GHRITLAHRE H.K., CHANDRAKAR P., AHMAD A.: *A comprehensive review on performance prediction of solar air heaters using artificial neural network*. Ann. Data Sci. (2019), 1–45.
- [43] GHRITLAHRE H.K., PRASAD R.K.: *Modelling of back propagation neural network to predict the thermal performance of porous bed solar air heater*. Arch. Thermodyn. **40**(2019), 4, 103–128.
- [44] AHMAD A., GHRITLAHRE H.K., CHANDRAKAR P.: *Implementation of ANN technique for performance prediction of solar thermal systems: A comprehensive review*. Trends Renew. Energ. (TRE)**6**(2020), 12–36. DOI: 10.17737/tre.2020.6.1.00110.